

# RADAR Scan Pattern synthesis and implementation on FPGA

S.Prathyusha(M.Tech)

Dr.D.Nageshwar Rao

**Abstract**— This paper presents an active and challenging areas of research in the field of Electronic Warfare(EW) and Pattern Recognition. Electronic intelligence (ELINT) is the result of observing the signals transmitted by radar systems to obtain information about their capabilities: it is the remote sensing of remote sensors. ELINT also provides information about defensive systems, which is important in maintaining a credible deterrent force to penetrate those defenses. In this context estimation of the of radar Antenna Scan Period (ASP) and recognition of the Antenna Scan Type(AST) is important measure in analyzing level of threat from the radar. Usually estimation of radar ASP and recognition of the AST is performed by human operators in the EW world. In this paper a algorithm is synthesized for radar scan pattern. The characteristic parameters of antenna scanning includes AST, ASP with other such parameters like Radio frequency (RF),Pulse Width(PW),PulseAmplitude(PA),Pulse Repetition Interval (PRI),Direction Of Arrival (DOA) and The classification different scan types such as circular scan, sector scan, helical scan, raster scan, conical scan is done using features extracted from the generated antenna scan patterns. Classification of the Angle Of Arrival (AOA).AST's is done using both parametric and non parametric techniques of the pattern recognition synthesized in MATLAB. AST of radar is found using four unique features of antenna scanning such as azimuth angle, elevation angle, degree of rotation and number of elevation bars. The verilog code for the recognition of antenna scan type is simulated in Xilinx ISE 14.3 and implemented on the Spartan 3 FPGA.

**Index Terms**— Antenna Scan Period (ASP) , Antenna Scan Type(AST) , Angle Of Arrival (AOA).Direction Of Arrival (DOA),Electronic Warfare(EW),Electronic Support(ES), *Electronic intelligence* (ELINT), Pulse Width(PW),PulseAmplitude(PA),Pulse Repetition Interval (PRI),Radio Detection And Ranging (RADAR), Radio frequency (RF).

## I. INTRODUCTION

Military operations are executed in an information environment where the electromagnetic (EM) spectrum is becoming increasingly more complex.

Different technologies and military doctrines have evolved as the use of the EM spectrum has expanded vastly in many different bands. Electronic warfare (EW) is an umbrella term used to define any activity that can control the spectrum, attack an enemy, or impede enemy assaults via the spectrum. The goal of EW is to deny the opponent the advantage of, and ensure friendly unimpeded access to, the EM spectrum[2, 3]. Signal intelligence (SIGINT) missions are employed on a daily basis in peace time to support EW operations during war time. Such missions are responsible for recording, analyzing, and forming parameter databases of EM emissions of particular importance.

This paper addresses the problem of radar antenna scan type (AST) recognition and propose an algorithm to estimate the radar antenna scan period(ASP) followed by AST classification. Both ASP and AST are vital for EW systems in emitter classification and for the timing of electronic counter measures [1].A change of AST is also crucial in determining threat levels from radar. Despite their importance, there is a paucity of studies in the open literature on automatic AST recognition because of the classified nature of EW work. The conventional solution to the problem in EW is to employ

human operator who listens to the radar tone generated by the received pulses. The operator guesses the AST and estimates its period with a stopwatch. The main contribution of this paper is the automation of this process through the development of a novel ASP estimation and AST classification technique based on signal warping (resampling) and pattern recognition. Automating the AST recognition process completely eliminates the need for a human EW operator..

The algorithm proposed in this paper for AST classification is not based on correlation techniques but, rather, based on pattern recognition. It also takes into account and handles the variability of the ASP for different radars and warps (resamples) each signal so that each period is represented by a fixed number of samples. In present problem, both the signal length (period) and its shape change (because of the position of the radar and the EW receiver) within one class of data, the measures of similarity are based on autocorrelation functions, characteristic points, genetic algorithms, artificial neural networks (ANNs), Markov models, etc.

The rest of this paper is organized as follows. Section II provides fundamental information about pulsed radar systems and their distinctive parameters. The primary focus is on AST and ASP. The basic ASTs are overviewed in Section III. Section IV explains the proposed algorithm in detail. The algorithm is validated with synthetic and real data and a compare

between four AST classifiers is presented. Section V concludes the paper.

## II. PULSED RADAR PARAMETERS AND ELECTRONICWARFARE

The type of radar considered in this study is conventional pulsed radar widely used in military applications for searching, detecting, and tracking airborne targets [10]. Accurate tracking is crucial for following a particular target (such as an aircraft) or an unresolved cluster of targets (such as an aircraft formation) as well as for efficient use of weapons against the target. Over the years, different types of volume search and target-tracking methods have evolved. These methods, usually periodic, are deployed in the various radar from different manufacturers with widely varying parameters [7].

The parameters that characterize a pulsed radar are its carrier frequency, bandwidth, pulsewidth (PW), pulse amplitude (PA), time and direction of arrival (ToA and DoA), pulse repetition interval (PRI), signal power, lobe duration, AST, and ASP [7]. Modern radars usually have multiple signal bandwidths.

Antennas are the crucial and indispensable parts of radar systems as they radiate and receive EM waves. Radar systems use a wide variety of antenna types, specialized for different applications and functionalities [9]. Since the coverage of the antenna beamwidth in azimuth and elevation is usually not sufficient for the radar's requirements, the antenna is steered, either electronically or mechanically, to the desired part of the space. Considering a hemispherical volume to be covered, the number of distinct steering positions for a mechanically-steered antenna is given by  $2\pi/\Delta\theta\Delta\phi$ , where  $\Delta\theta$  and  $\Delta\phi$  are the azimuth and elevation beamwidths, respectively. This formula is not valid for electronically-scanned planar phased arrays since the beam broadens in angle (although it remains invariant in sine space). The EW receiver tries to acquire information about radar in the environment (and possibly jam them) to protect the platform on which it is located while the platform performs its mission. In systems that detect ToA, PA, and duration, many options for antenna scan analysis are available. The approach we have taken in this work for scan analysis is based on measuring the PA and estimating the ASP in the time domain in order to determine the AST. PA is the received signal power of the pulse at the EW antenna and is given by

$$P_r(t) = \frac{P_t G_r \lambda^2}{4\pi R^2} G_t(\theta(t), \phi(t)) \quad (1)$$

where  $P_r$ , and  $P_t$  are the transmitted and the received power,  $G_r$  is the receiver antenna gain,  $\lambda$  is the wavelength,  $R$  is the range between the radar and the EW receiver, and  $L$  is the loss factor. Atmospheric propagation losses are proportional to range and frequency and can be significant for low elevation angles which are commonly encountered. Polariza-

tion mismatch between the two antennas is another factor that affects the PA. As the antenna rotates to different parts of the volume, the received power changes according to the gain of the antenna at the angular position of the EW receiver. Hence,  $G_t(\theta(t), \phi(t))$  is the radar transmitter antenna gain at the azimuth and elevation angles where the EW receiver is located at time  $t$ . The term  $\frac{P_t G_r \lambda^2}{4\pi R^2}$  is assumed to be constant because the geometry (range and angle) between the radar and the EW receiver is assumed to be changing negligibly. This assumption is valid for stationary engagement scenarios and scenarios where the scan rate of the antenna is much faster than the motion of the system platform, which is mostly the case in EW. When the relative motion between the radar and the EW receiver is significant, this assumption is no longer valid, the range  $R$  becomes time dependent, and the received signal power in (1) becomes a function of the changing  $R$ . Assuming that it is possible to constantly update the positions of the radar and the EW receiver through the use of geolocation, the range  $R$  can be recalculated at each scan and used in (1). It is also possible to calibrate the radar system to measure velocity together with range to exploit Doppler information. If the received power is above the sensitivity level of the EW receiver, radar pulses with different amplitudes are detected and analyzed. The sensitivity level of the receiver depends on its bandwidth and noise figure. The ASP is the shortest time interval between the repetitive patterns observed in a PA recording. Instead of the ASP, sometimes the antenna scan rate (ASR) is used, which is simply the reciprocal of the ASP. When the ASP is short so that the ASR is large (as is the case for conical scans for example), the latter is stated more often because of the convenience of numerical representation.

## III. BASIC ANTENNA SCAN TYPES

Radars use different search-and-track strategies to cover the specific region they are directed to. These strategies determine the radar's AST. The basic ASTs are described in [7], [9] and are summarized below.

**1) Circular Scan:** The circular scan is widely used in search radars. The radar scans the complete azimuth plane ( $360^\circ$ ) at a constant angular speed (Fig. 1). The antenna typically has a large elevation beamwidth, called a fan beam, to cover the whole elevation space without having to scan it. The EW receiver samples the PA with a sampling period equal to the PRI since the pulses are received with PRI intervals in time. The ASP has quite a large range, on the order of 1–10 s.

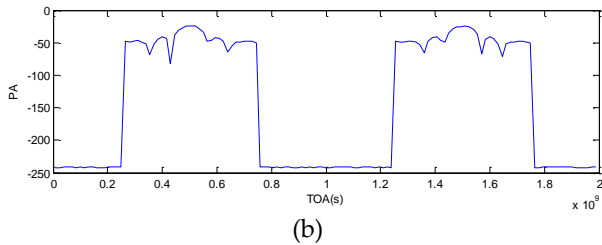
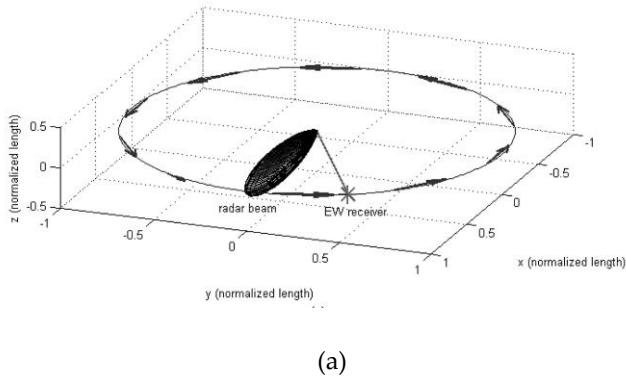


Fig. 1. Circular scan. (a) Main beam positions. (b) PA versus ToA graph, where solid dots indicate measured PAs.

**2) Sector Scan:** In the sector scan, the radar sweeps a specific angular sector back and forth at constant angular speed (Fig. 2(a)). The EW antenna receives periodic and symmetric main beams, as shown in Fig. 2(b). Two main beams with equal peaks are expected for each full period. The ASP is on the order of seconds.

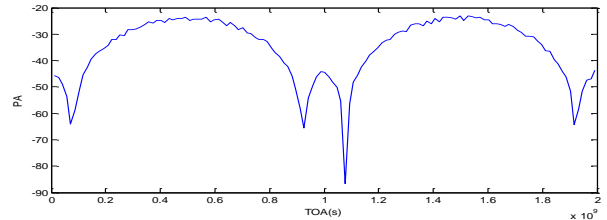


Fig. 2. Sector scan. (a) Main beam positions. (b) PA versus ToA graph.

constant and in each full period, a main beam is intercepted for each bar of the raster scan. However, since the elevation is also changing in this scan type, the received PA varies with the elevation of the EW receiver.

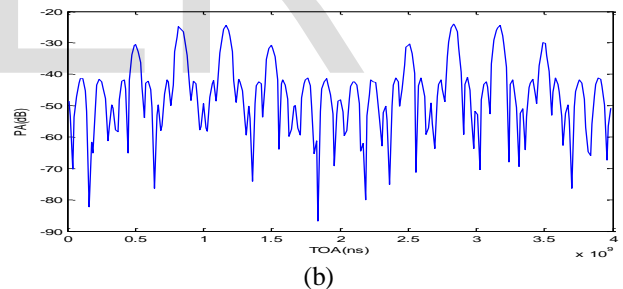
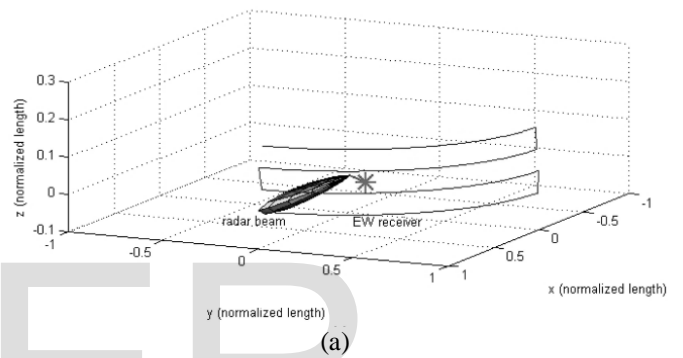
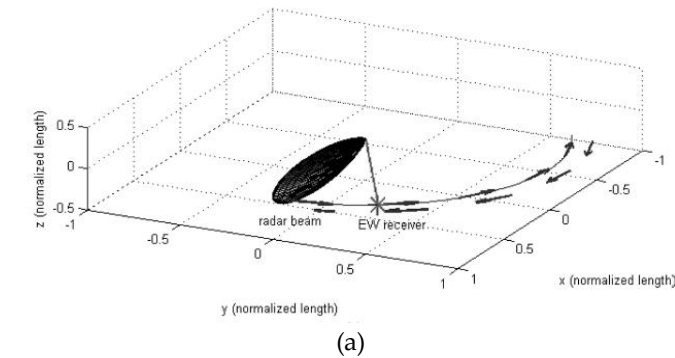


Fig. 3. Raster scan. (a) Main beam positions. (b) PA versus ToA graph.



**3) Raster Scan:** The two scan types described above search only in azimuth, but the raster scan searches both in azimuth and elevation (Fig. 3). The radar scans a specific angular sector in azimuth and increments its elevation after completing the sector, similar to the raster scan on TV screens. There can be several elevation levels. Figure 3 shows the antenna motion and the received PA as a function of ToA. The period is

**4) Helical Scan:** In the helical scan, the radar revolves  $360 \pm$  several times while the elevation changes continuously so that the radar scans a specific sector in elevation. After a complete scan period, the elevation is set back to where the scan began. The shape of the scan resembles a helix (Fig. 4). The received PA versus ToA signal (Fig. 4(b)), is similar to the circular scan except that the peaks of the pattern change because of the motion in the elevation plane.

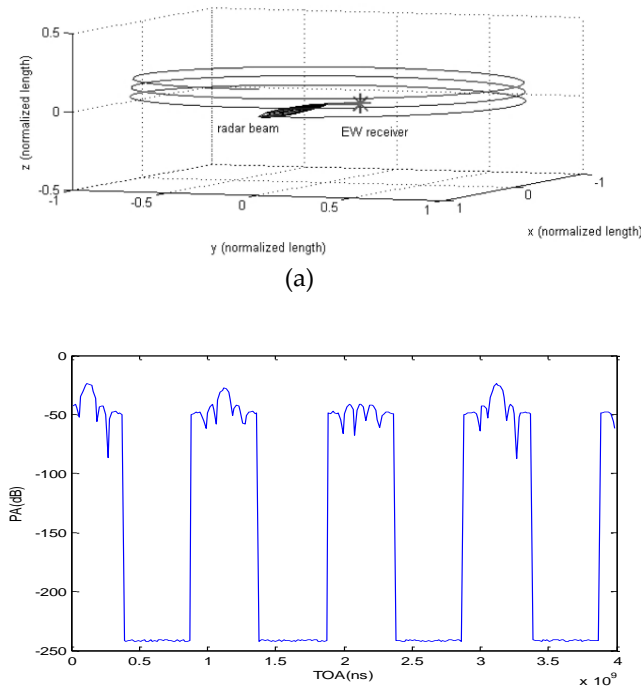


Fig. 4. Helical scan. (a) Main beam positions. (b) PA versus ToA graph.

**5) Conical Scan:** A critical piece of information in scanning is whether radar is tracking the platform the EW receiver is located on. A conical scan indicates that radar is trying to lock onto the platform by scanning conically around it to place it on the 3 dB beamwidth. Figure 5(a) illustrates the movement of the antenna. The received signal, illustrated in Fig. 5(b), is initially a sinusoid because the beam travels closer to, then farther from the EW receiver. As the lock improves, the amplitude of the sinusoid decreases. The period of the sinusoid is distinct for each type of radar. Eventually, when the radar is locked completely, the track process converges to a perfect track. In other words, when the platform is right on the 3 dB beamwidth, the received PA becomes constant. The complete lock of this scan type is sometimes called a fixed scan. The PA during the locking-on process is illustrated in Fig. 5(c). Other antenna scan types are bow tie scan and Archimedes spiral type scan, which are not as common as those described above. These are not considered in this study. Unlike radars that have basic preprogrammed scan types, as those considered in this paper, phased-array radars have very complex and dynamic beam management algorithms. A phased array may be used to generate a fixed radiation pattern, or to scan rapidly in azimuth or elevation. Modern phased-array radars rely on digital beamforming and employ track-while-scan algorithms that dynamically change the beam formation of the radar according to the received pulses, threat location and speed, etc. Therefore, the beam shape of phased-array radars change with the steering angle. The beamwidth is approximately inversely proportional to the angle measured from the normal to the

antenna [18]. In addition to the changing shape of the main beam, the sidelobes also change in appearance and position. Consequently, the antenna scan pattern received at the EW receiver keeps changing, complicating the ASP estimation and AST recognition problem. Instead of ASP and AST, one can use lobe duration (illumination time) as a distinctive feature of phased-array radars. However, one should consider that the lobe duration may also vary (probably small variations) because of the beam broadening nature of phased arrays when looking off the boresight of the array.

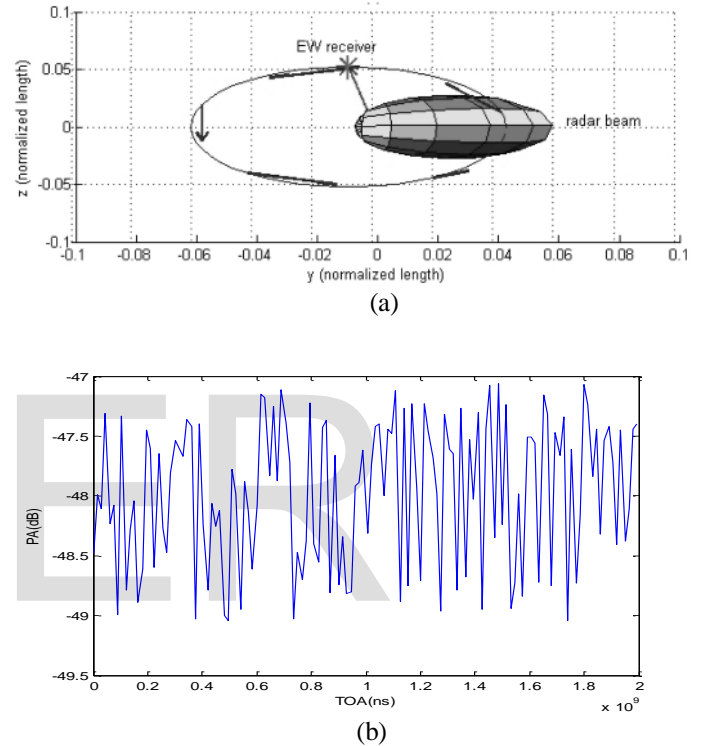


Fig. 5. Conical scan. (a) Main beam positions. (b) PA versus ToA graph.

#### IV. AST RECOGNITION ALGORITHM

The AST recognition problem can be summarized as estimating the relative angular position of the EW receiver with respect to the radar main beam as time passes, and classifying the radar AST into one of the most frequently encountered scan patterns.

##### A. The Input Signal

The input PA versus the ToA data is the real data acquired by the EW receiver. Figure 6 shows an example PA versus a ToA signal from a circular scan where each period is shown. Since the output from these source are in dBW (decibel relative to Watt), the signal is first transformed from dBW to Volt (V) scale using

$$voltage = 10^{(power/20)} \quad (2)$$

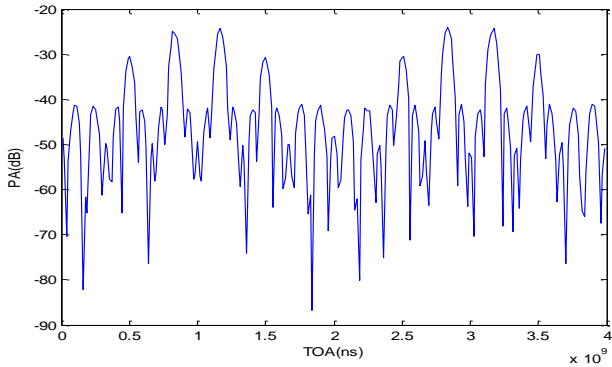


Fig .6. An example PA versus a ToA signal from a circular scan

**B. Period Estimation**

A continuous-time signal  $x(t)$  is called periodic if  $x(t) = x(t+T)$  for some period value  $T$ . The smallest value of  $T$  that satisfies this equality is called the fundamental period. Frequency-domain methods estimate the period by detecting the peaks of the frequency spectrum. This approach possesses some problems when the signal is not a sinusoid, but has a wide bandwidth. In this case, the peaks may be illusive when estimating the fundamental frequency.

Time-domain methods are particularly useful for period estimation of nonsinusoidal signals. These methods define some kind of similarity metric and try to maximize the similarity with the lagged versions of the signal using this metric. For example, the average magnitude difference or the autocorrelation between the signal and its lagged versions can be used as similarity metrics. The lag value where the similarity is maximized corresponds to the period estimate of the signal. The backbone of the algorithm is the ASP estimation, which affects the overall performance of AST classification significantly. In this study period estimation is performed by using the normalized autocorrelation.

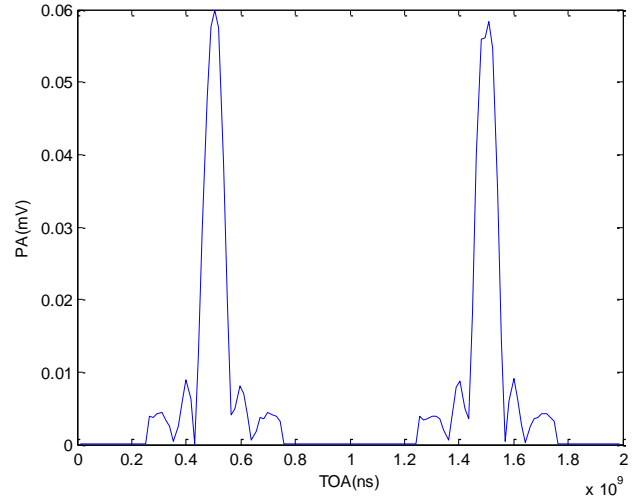


Fig. 7: Transformed signal ready for period estimation.

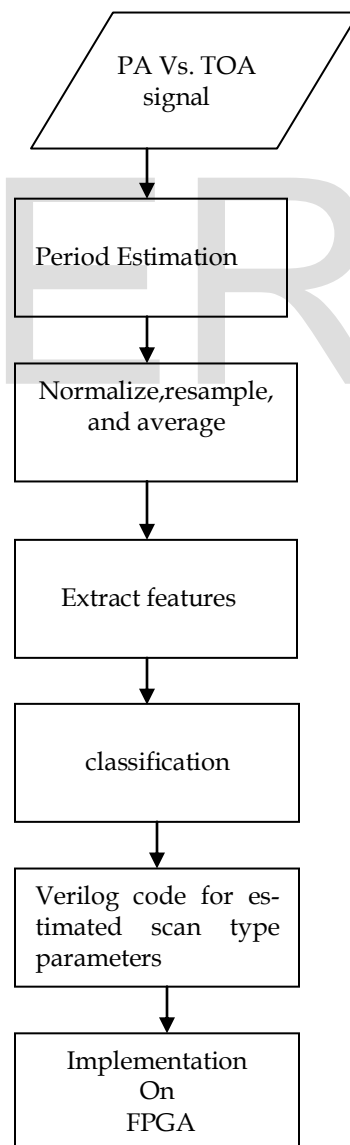


Fig. 8. An overview of the proposed algorithm



**C. Preprocessing (Normalization, Resampling, and Averaging)**

This part prepares the signal for the feature extraction phase by normalizing, averaging, and finally resampling the signal. The normalization process is quite simple where the signal is simply scaled by its maximum value so that the signal varies between 0 and 1:

$$x_{norm}[k] = \frac{x[k]}{\max(x[k])} \quad k = 0, 1, \dots, L - 1 \quad (3)$$

This process tries to remove the effects of propagation, since propagation results in a decay in pulse amplitude, proportionate to the distance between the radar and the EW receiver. Here, we are not concerned with the distance and rather concerned with the antenna scan type which is independent of constant decays. Fig. 9. shows the normalized autocorrelation coefficients calculated for the signal.

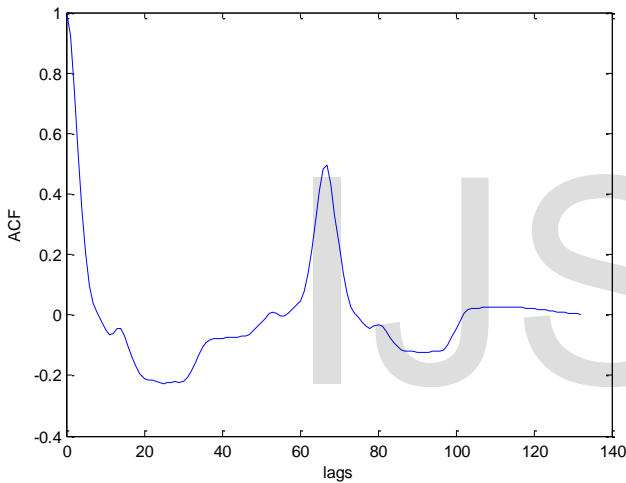


Fig. 9: Normalized autocorrelation coefficients calculated for the signal.

Next, we resample the signal so that the total number of samples from one cycle of a particular scan type is  $N$  where the value of  $N$  depends on the signal. This process transforms all of the recorded signals from different radars with different PRIs, different ASTs and different ASPs with  $T/T_s$  elements into a standard signal vector with  $N$  elements. Here,  $T$  is the estimated period and  $T_s$  is the sampling interval of the original signal. The process also regularizes the different sampling periods of the signal to  $T/N$ . The value of  $N$  is chosen as 2000 throughout the example signal. This resampling phase also reduces the amount of data because radars use much larger number of pulses per scan period to be aware of the environment, so it becomes a decimation operation. Since a high sampling rate is available before the resampling phase, nearest point interpolation technique can be used with negligible distortion in the signal. This process was defined in Equation (3). Assuming  $M$  full cycles of signal are available to estimate the period of the signal, the signal can coherently be averaged

using Equation (4.4) to decrease the effect of noise. Figure 4.7 shows the signal with the periodic parts.

**D. Feature Extraction**

In this section, we describe the four features selected and used by the algorithm. Input to this part is the preprocessed  $N$  element signal with sampling interval  $T/N$ .

There are a total of 100 data points, 20 from each of the following scan types in the following order: circular, sector, raster, helical, and conical. These signals are synthesized by using the ASPs described in the previous chapter. The parameters (azimuth and elevation beamwidths, sector width, number of bars in raster, scan period etc.) used while generating the signals are very important. The results of the classification phase could be very misleading if the parameters are not set appropriate with the real world examples. Therefore, we have used a classified database which the parameters of the radars are accountable on and have selected these parameters accordingly. We have attempted to use a number of different features such as the mean, standard deviation, and skewness, but the best results were obtained with the four features described below:

**Kurtosis of the Signal**

Kurtosis is the normalized fourth-moment of a random variable  $X$  and is defined as:

$$kurtosis = \frac{E[X - \mu]^4}{\sigma^4} \quad (4)$$

where  $\mu$  is the mean and  $\sigma$  is the standard deviation of the random variable.

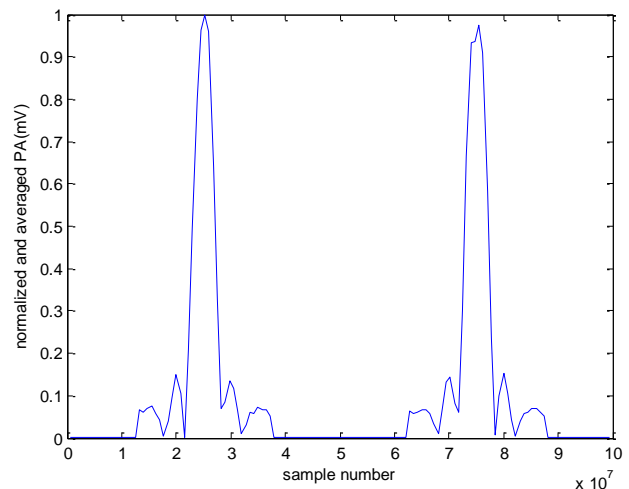


Fig. 10: Full periods in the signal.

Kurtosis is a statistical measure of how peaked or how flat the distribution of the random variable is. It can also be seen as a measure of how heavy the tails of the distribution are relative to the Gaussian distribution which has a kurtosis value of 3. Concentrated distributions such as the uniform distribution have kurtosis values less than 3. If the distribution

has heavier tails and is more outlier prone, its kurtosis value exceeds 3. In track modes, radars try to illuminate the threat as much as possible so that they can update the threat's coordinates finely and accurately for a possible attack. To perform this task, they have to steer the beam such that it is on the platform all of the time. This in turn means that the EW receiver will get all the pulses of the radar with slight differences in amplitude (i.e., a narrow distribution of amplitude) depending on the track scanning type of the radar system. The amplitude variation is approximately uniform. A conical scan signal, which is a uniformly sampled sinusoid, has a kurtosis value of around 1.5. By looking at the signal's kurtosis value, the system will get an idea about its mode and scan. The kurtosis value will be small for conical scan and large otherwise. The kurtosis is selected as the first feature:

$$F1 = \text{kurtosis}(x[k]) \quad (5)$$

### Cross Correlation of the Signal with the Main Beam

It can be observed by analyzing different scan types and their effect on the EW platform that the position of the main beam differentiates the scans from each other. The phenomenon behind the data reveals this information very clearly. The radar is trying to search different volumes of space with different periodic strategies. So the relation of the time between the main beams and the amplitude variation of the main beams are the key parameters for a robust recognition system. First, the algorithm has to detect the main beam in the signal. This can be achieved quite easily by finding the maximum point in the signal. Assuming that there is a main beam in the signal, this has to be the maximum point. From the index of the maximum point, it starts to advance indices until the magnitude drops to 0.01. The process is repeated exactly in the same way for the pulses previous to the maximum point. By using these two points neighboring the maximum point where the amplitude drops to 0.01, it extracts the main beam between these two points. Figure 4.10 illustrates the signal and the main beam detected in the signal. After finding one of the main beams in the signal, the algorithm detects all of the possible main beams in the signal by using the normalized cross correlation between the signal and the main beam found. The normalized cross correlation between two discrete sequences  $x[n]$  and  $y[n]$  is defined as follows:

$$r_{xy}[k] = \frac{\sum_{i=0}^{V-1} x[i]y[i+k]}{\sqrt{\sum_{i=0}^{V-1} x^2[i]} \sqrt{\sum_{i=0}^{V-1} y^2[i+k]}} \quad (6)$$

where  $V$  is the length of the main beam vector. Setting a threshold (0.95 is used in this study) and finding the peaks in the cross correlation values gives all the possible main beams. One would expect the cross correlation value to be large since the patterns of different antennas are very similar near their bore sights. For scan types where no elevational action is involved (circular and sector), the main beams will be exactly the same, ignoring the effect of noise. The threshold can be

tuned according to the signal to be able to handle the possible variations in the azimuth pattern caused by the changing elevation angle. After finding the possible main beams in the signal, some very important relations are calculated from the time position and the pulse amplitudes of the main beams. The number of main beams is an important parameter that can differentiate some scan types from the others. In particular, the circular scan has only one beam in one period which is a valuable feature to discriminate it from the others. Circular and sector scan types are very visible in the figure by this parameter. It can also be seen that no main beam is found in the conical signal since the pulse variation is not observed. Therefore, we choose the second feature as the number of main beams:

$$F2 = \text{number of main beams in the signal} \quad (7)$$

Amplitude variation of the main beams can also be a very useful feature. The range of the main beam amplitudes is used as a measure of the variation by subtracting the minimum amplitude from the maximum amplitude. This feature can differentiate between azimuthal and elevational scan types. More generally, this feature can differentiate the scan types that involve only one plane (azimuth) and the ones that scan both planes (azimuth and elevation). Therefore, the third feature becomes the amplitude variation of the main beams:

$$F3 = \max(\text{main beam PAs}) - \min(\text{main beam PAs}) \quad (8)$$

One can see that the variation could not be calculated for circular scan types since this type of scan produce only one main beam. Similarly, since the conical scan does not have any distinct main beam, variation of main beams is not calculated as well. However, it is observed that the sector scan type can be separated from the others with this feature.

Time difference between the main beams is also a distinctive parameter between classes. Circular and helical scan types revolve the 360° sector continuously without going back and forth like sector and raster scans. In this case, one expects to see the time difference between the main beams to be very similar. However, in the raster scan, the time difference between the main beams should vary most of the time because of the nature of the scan. The only case where the time difference will be the same is when the EW receiver is in the middle of the scanned sector which is unlikely.

For this,  $\max(\text{time differences}) / \min(\text{time differences})$  is calculated and used as a parameter. We observe that this feature is only calculable for helical and raster scans since there should be at least three main beams to calculate the variation of time differences between the main beams. Therefore, the final feature is chosen as the variation of the time differences:

$$F4 = \frac{\max(\text{time differences})}{\min(\text{time differences})} \quad (9)$$

**E.Classification**

The above features are used in the classification phase. For features that cannot be calculated for different scan types, 1000 value is used as a numeric value for the classification algorithm input as an indicator. For example, a main beam cannot be observed in a conical scan so its features other than the kurtosis cannot be calculated and set as 1000 to ease the calculations in the classification part. Four different classification techniques are used: naive Bayes, decision tree, multilayer perceptron neural network, and support vector machines. The classification rates according the *N* parameter of the algorithm is shown to see the effect of the number of samples per period. The classification methods and their results are presented below. An open source machine learning software WEKA, developed by The University of Waikato, is used in the classification process [16]. We have used 4-fold cross-validation technique for training and testing the algorithm. In this cross-validation technique, the data points from each class are randomly partitioned into four groups. In the first run, first part is retained for testing and the remaining is used for training. In the second fold, the second part is retained for testing and the remaining is used for training. All of the data points are tested by this procedure by repeating this procedure four times.

**1) Naive Bayes**

Naive Bayes classifier classifies according to the Bayes' theorem. The classifier calculates the posterior probabilities according to the models of each class. The decision rule for classification is merely picking the hypothesis that is more probable.

Assuming  $w_1, w_2, \dots, w_n$  are the classes,  $p(x|w_j)$  is the state-conditional density function assuming that the given class is  $w_j$ , then the posterior probability is calculated as follows:

$$p\left(\frac{w_j}{x}\right) = \frac{p\left(\frac{w_j}{x}\right)p(w_j)}{p(x)} \tag{10}$$

Where  $p(x) = \sum_{j=1}^n p\left(\frac{w_j}{x}\right)p(w_j)$  is the total probability.

In the training phase, probability models for  $p\left(\frac{x}{w_j}\right)$  are calculated using the training signal for each  $w_j$ . The probability density function is assumed to be a normal distribution and the parameters of the distribution are calculated by maximum likelihood estimation. In naive Bayes method, each of the features are assumed independent and the calculations of the parameters of the model are made accordingly. This assumption greatly simplifies the calculations and the complexity of the model. The classification phase calculates the posterior probabilities according to Equation (10). The class of the signal is chosen as the most probable class according to the calculated posterior probabilities [13]. It can be seen that for very small

*N*, the signal is undersampled and the features are not correctly extracted, causing errors in the classification. One can conclude from the figure that *N* = 1000 is a good choice in terms of the correct classification rate and computational complexity.

Table 1: Confusion matrix for the naive bayes classifier with correct classification rate.

		Classification results				
		circular	sector	raster	helical	conical
True class	circular	10	3	0	0	0
	sector	3	0	0	0	0
	raster	1	0	0	0	0
	helical	1	0	0	0	0
	conical	2	0	0	0	0

**2) Decision Tree**

Decision trees are the most intuitive and natural way of classification [13]. One finds a sequence of test questions starting from a main question and branches all the way to a terminating node where the class of the signal is found. The structure of our problem fits well into a decision tree like structure since each one of the selected features is discriminative for one or two of the scan types. That is, if one knows that the kurtosis value is low, than it is highly probable that it is a conical scan. There are quite a lot of different tree growing algorithms that use training signals and establish a tree which classifies the signal. The most popular ones are: Classification and regression trees (CART) and C4.5. More information about these algorithms can be found in [13] with an extensive explanation. Besides the algorithms mentioned above, a relatively newly proposed best first tree (BFTree) learning algorithm is also considered in this study. It is seen that this algorithm comes up with trees that can classify the scans more accurately. The following results are obtained by using the BFTree algorithm. More information about this algorithm can be found in [13]. The same undersampling effect seen in the previous classifier is also seen here with *N* = 1000 being a suitable choice. The confusion matrix for the decision tree when *N* = 1000 is used is given in Table 2.



Table 2: Confusion matrix for the decision tree classifier with correct classification rate.

		Classification results				
		circular	sector	raster	helical	Conical
True class	circular	13	0	0	0	0
	Sector	3	0	0	0	0
	Raster	1	0	0	0	0
	helical	0	0	0	0	1
	conical	1	0	0	1	0

### 3) Artificial Neural Networks

Artificial neural networks (ANN) are classifiers that try to emulate the computational processes in the human brain. They consist of nodes similar to the neurons in the nervous system. The interconnection between nodes is only through-weighted sums of the inputs of the neuron. In the neuron itself, a non-linear function called the activation function, is used to model the process in the neuron. There are usually three types of layers in an ANN: an input layer, one or more hidden layers, and an output layer. The input layer has sufficient number of nodes to cover the inputs; the output has also nodes to represent the outputs. The part where the patterns are learnt are the hidden layers of the system. The number of hidden layers and the number of nodes in each hidden layer can be chosen by the designer. Small number of neurons in the hidden layer may not satisfy the user in terms of classification accuracy because the ANN may not be able to learn the patterns sufficiently. However, an excess of neurons in the hidden layer causes a lot of complexity in the training part and it also could lead to "memorization" of the signal instead of "learning" the dynamics of the signal. Due to the presence of distributed nonlinearity and a high degree of connectivity, theoretical analysis of ANNs is difficult. The performance of ANNs is affected by the choice of parameters related to the network structure, training algorithm, and input signals, as well as by parameter initialization [14]. There is a variety of different networks, training methods, and activation functions for different types of applications [14]. A multi-layer (three layer) perceptron with a back-propagation algorithm is used in this study. This is a supervised method which uses a gradient-descent algorithm based on the error at the output. It tries to minimize the error by feeding back the error at the output to update the weights in each epoch. After the network is trained, classification is performed: the inputs are fed to the ANN with the already converged weights and the class of the signal is determined according to the output. The classification results with respect to  $N$  is depicted in Figure 4.20. The effect of undersampling and the saturation after a point is also seen in this figure as in the previous classifiers. The confusion matrix for the ANN classifier when

$N = 1000$  is given in Table 4.5.

Table 4.5: Confusion matrix for the ANN classifier with correct classification rate.

		Classification results				
		circular	sector	raster	Helical	conical
True class	circular	10	3	0	0	0
	sector	3	0	0	0	0
	raster	1	2	0	0	0
	helical	0	0	0	0	1
	conical	0	0	1	0	1

### 4) Support Vector Machines

Support Vector Machines (SVMs) is a binary classifier that tries to divide the space with hyperplanes where each volume represents a different class. The hyperplane that is expected to be found is a hyperplane that maximizes the margin of separation between the classes. The hyperplane is found by using the data points that are between the classes. These points are very valuable in separating the classes and are called the support vectors. By using these points and by the help of quadratic programming, the hyperplanes that separate the classes are found. If a hyperplane is not sufficient to divide the classes, i.e., the region dividing classes is not linear, one can use different kernels to transform the signal to different spaces [7].

In this study, a linear SVM is trained with the signal without any kernel and one-versus-the-rest classification is performed since there are more than two classes. The cases where  $N < 1000$  did not converge. The confusion matrix for the support vector machine when  $N = 1000$  is used is given in Table 2.

Table 4: Confusion matrix for support vector machine classifier with correct classification rate.

		Classification results				
		circular	sector	raster	Helical	conical
True class	circular	13	0	0	0	0
	sector	3	0	0	1	0
	raster	1	0	0	0	0
	helical	0	0	0	0	1
	conical	0	0	0	0	2

### Comparison of the Computational Time of the Classifiers

We have also analyzed the time it takes to train and test the classifiers used in the study as an indication of computational complexity of each classifier. The results obtained with WEKA, given in Table 5, shows us that the decision-tree classifier outperforms the other classifiers in terms of computational complexity as well.

Table 5: Amount of time needed for training and testing for each classifier.

classifier	Time(s)
Naïve Bayes	0.03
Decision tree	0.02
ANN	0.19
SVM	1.03

The robustness against noise presented in the previous sections and low computational complexity of the decision-tree classifier indicates that for this particular application, decision tree is the most suitable choice as a class.

#### F) Synthesis of estimated scan type parameters

A design for the estimated parameters of the different scan types is synthesized in the Xilinx ISE design suite and simulated in the ISIM of Xilinx ISE 14.3.

#### G) Implementation on FPGA.

The simulated code is implemented on the SPARTAN 3 FPGA kit.

## V. CONCLUSIONS

Paper addressed the problem of radar ASP estimation and AST classification in EW signal processing on which no clear and accessible study is available in the open literature. The research for an automatized solution to the problem led to a sufficiently general algorithm that uses the conventional parameters of radar systems. The main contribution of this work is the design of a novel and robust algorithm for AST classification.

Future work involves modifying the algorithm so that it can operate in real time as the radar signal is acquired by an EW receiver. The main difficulty here would be to differentiate the sidelobes from the mainlobe when only partial data is observed instead of the whole.

## REFERENCES

[1] Neri, F. *Introduction to Electronic Defense Systems* (2nd ed.).

Norwood, MA: Artech House, 2001.

[2] Wikipedia [http://en.wikipedia.org/wiki/Electronic\\_warfare](http://en.wikipedia.org/wiki/Electronic_warfare).

[3] Wiley, R. G. *ELINT: The Interception and Analysis of Radar Signals*. Norwood, MA: Artech House, 2006.

[4] Greer, T. H. Automatic recognition of radar scan type. U.S. Patent 6,697,007, 2004.

[5] Mahafza, B. R. *Radar Systems Analysis and Design Using MATLAB*. Boca Raton, FL: Chapman & Hall/CRC Press, 2000.

[6] Skolnik, M. I. *Introduction to Radar Systems* (3rd ed.). New York: McGraw-Hill, 2000.

[7] Skolnik, M. I. (Ed.) *Radar Handbook*, (3rd ed.). New York: McGraw-Hill, 2008.

[8] United States Navy *Electronic Warfare and Radar Systems Engineering Handbook*. Naval Air Systems Command, Avionics Dept., Washington, D.C., 1999.

[9] Balanis, C. A. *Antenna Theory Analysis and Design* (3rd ed.). Hoboken, NJ: Wiley, 1997.

[10] Stimson, G. W. *Introduction to Airborne Radar* (2nd ed.). Raleigh, NC: SciTech Publishing, 1998.

[11] Adamy, D. L. *Introduction to Electronic Warfare: Modeling and Simulation*. Raleigh, NC: SciTech Publishing Inc., 2006.

[12] Eravcg, B. Automatic radar antenna scan analysis in electronic warfare. Master's thesis, Bilkent University, Dept. of Electrical and Electronics Engineering, Ankara, Turkey, Aug. 2010.

[13] Theodoridis, S. and Koutroumbas, K. *Pattern Recognition* (4th ed.). Burlington, MA: Academic Press, 2009.

[14] Haykin, S. *Neural Networks and Learning Machines* (3rd ed.). Upper Saddle River, NJ: Prentice-Hall, 2009.

[15] Shawe-Taylor, J. and Cristianini, N. *An Introduction to Support Vector Machines and Other Kernel-Based Learning Methods*. New York: Cambridge University Press, 2000.

[16] Hall, M., et al. The WEKA data mining software: An update. *ACM SIGKDD Explorations Newsletter*, 11, 1 (June 2009)10-18, <http://www.cs.waikato.ac.nz/ml/weka/>.

[17] Witten, I. H. and Frank, E. *Data Mining: Practical Machine Learning Tools and Techniques* (2nd ed.). San Francisco, CA: Morgan Kaufmann, 2005.

[18] Xilinx Isim In-depth tutorial from the dov-nav of the Xilinx ISE 14.3 design suite.

[19] NPTEL sources, video lectures on Pattern recognition and applications by P.K. Biswas, IIT kharagpur.

[20] MATLAB r2013 a tool boxes: NN pattern recognition tool box, phased array system toolbox.